Journal Name

New Journal of Chemistry

Dynamic Article Links ▶

ARTICLE TYPE

Fabrication of copper sulfide using a Cu-based metal organic framework for colorimetric determination and efficient removal of Hg^{2+} in aqueous solutions

Yuhao Xiong, Linjing Su, Haiguan Yang, Peng Zhang, Fanggui Ye[*]

CuS particles (PCuS) were facilely synthesized by wet-treatment of a Cu-based metal organic framework (HKUST-1). PCuS possesses an impressive intrinsic peroxidase-like activity. As a result of this affinity, PCuS readily binds to 3,3′,5′,5-tetramethylbenzidine (TMB) in the presence of hydrogen peroxide (H_2O_2)
10 (K_m values of 29 μM and 150 μM toward TMB and H_2O_2, respectively). Interestingly, when Hg^{2+} was added, the HgS produced in conjunction with the specific binding sites on the surface of PCuS remarkably inhibited the peroxidase-like activity of PCuS. On the basis of this unique property, a sensing platform for the colorimetric detection of Hg^{2+} was established. In addition, high surface area and strong affinity to Hg^{2+} makes PCuS an excellent adsorbent for Hg^{2+} (2105 mg g^{-1}). These results indicate that
15 PCuS using HKUST-1 as a precursor could be a useful material for the facile detection and efficient removal of Hg^{2+} in environmental abatement applications.

Introduction

With the rapid development of nanoscience and related technologies, copper-based nanomaterials are playing an
20 important role in industries such as printed electronics[1], semiconductors [2], and imaging and sensing devices [3]. One such material, copper sulfide (CuS), has attracted considerable attention due to its unique optical, photovoltaic, catalytical, and many other properties [4]. Many methods have been developed to
25 synthesize CuS, including thermolysis, microwave irradiation, and template-assisted methods. Most of them, however, have disadvantages, such as high-temperature requirements, air-free conditions, or elaborate and costly synthesis routes [5]. Therefore, a simple new method for the fabrication of CuS is needed.
30 Metal-organic frameworks (MOFs) are a fascinating new class of crystalline porous materials that have emerged in the past decade[6]. MOFs have attracted much attention in building inorganic materials nanostructures[7] thanks to their high surface area, diverse porosity, and customizable chemical properties. For
35 example, CeO$_2$ [8], Co$_3$O$_4$ [9], ZnO [10], and CuO [11] have been synthesized using MOF templates. MOF-derived functional inorganic materials have demonstrated several advantages. These include: 1) ability to transform many inorganic compounds into nanomaterials based on the wide variety of MOFs available, 2)
40 high surface area, and 3) a large variety of possible pore sizes [12]. Using MOFs, inorganic nanomaterials with new properties, and expanded capabilities can be synthesized compared with their traditionally built counterparts. However, although MOFs are good templates for fabricating inorganic materials, the costly
45 carbonization process limits their large-scale preparation and

application. Recently, an encouraging breakthrough in synthesizing inorganic materials using MOFs as a precursor has been achieved by Lin's group [13,14]. They reported a simple wet-treatment method of fabricating porous indium sulfide and
50 zirconium phosphate, which showed good performance for lanthanide and heavy metals extraction. This method is easy to operate and does not require complicated ligand synthesis and activation steps.

Mercury ions (Hg^{2+}) pose a significant threat to the environment
55 and public health. The United States Environmental Protection Agency (EPA) has established a maximum allowable concentration of 10 nM in drinking water [15], which is a minuscule quantity. Hence, the efficient removal of Hg^{2+} from the environment is recognized as a top priority by the World Health
60 Organization [16]. A convenient, effective, and rapid method for Hg^{2+} monitoring and removal in water has, thus, become a top global priority. Colorimetric sensors are low-cost, simple, and practical devices for effectively monitoring Hg^{2+}, for which recent improvements have been demonstrated [17]. In other
65 developments, high-adsorption materials are improving the ability to collect Hg^{2+}. Thiol-functionalized porous materials possess an excellent ability for Hg^{2+} adsorption due the strong affinity of Hg^{2+} and S-containing ligands. However, most of the reported colorimetric sensors for Hg^{2+} detection were based on
70 the high cost of noble metal nanoparticles (such as Au and Pt). In addition, the preparation process of these nanoparticles was tedious and time-consuming, and complex purification procedures were also necessary [15,18-21]. Moreover, a tedious post synthetic method was often used to modify thiol-functionalized
75 porous materials for Hg^{2+} adsorption [22]. This reality prompted us to consider the feasibility of developing a method for the rapid

preparation of porous CuS directly acting as both an Hg^{2+} detection platform and an adsorbent.

Encouraged by this possibility, we pursued the synthesis of CuS particles using HKUST-1 as a precursor through a facile wet-
5 treatment method (designated as PCuS). Our synthesized PCuS demonstrated high catalytic activity in terms of mimicking peroxidase activity and excellent adsorption capability toward Hg^{2+} without any post synthetic modification. As expected, Hg^{2+} showed remarkable inhibition of the peroxidase-like activity of
10 PCuS (similar to poisoning catalysts). Based on this interesting phenomenon, a colorimetric platform for detection of Hg^{2+} with good sensitivity, selectivity, and rapidity was constructed. All things considered, our results suggest that the synthesized PCuS particles may be used as a peroxidase mimic for Hg^{2+} detection
15 and also as an excellent adsorbent for Hg^{2+} removal. This capability of PCuS particles will likely expand the scope of applications for HKUST-1.

Experimental section

Reagents and materials

20 Cu $(NO_3)_2 \cdot 3H_2O$, 1,3,5-benzenetricarboxylic acid (H_3BTC) and anhydrous ethanol were purchased from Shanghai Chemical Reagents Corporation (Shanghai, China). Sodium sulfide nonahydrate ($Na_2S \cdot 9H_2O$) and a hydrogen peroxide solution (30 wt% H_2O_2) were provided by Shantou Xilong Chemical Factory
25 (Guangdong, China). 3,3',5,5'-tetramethylbenzidine (TMB) was purchased from TCI (Shanghai, China). $HgCl_2$ was supplied by J&K Scientific (Beijing, China). Other reagents were obtained from Aladdin Chemistry Co. Ltd. (Shanghai, China). Ultrapure water was produced by a Millipore purification system (Bedford,
30 MA, USA) and was used to prepare all aqueous solutions.

Characterizations

Powder X-ray diffraction (XRD) patterns were performed on a D/max 2550 VB/PC diffractometer (Rigaku, Japan). Fourier transform infrared (FT-IR) spectra (4000–400 cm^{-1}) were
35 recorded in KBr discs on a PE Spectrum One FT-IR spectrometer (Perkin Elmer, USA). Raman spectra were recorded on an inVia spectrometer (Renishaw, UK). Thermogravimetric analysis (TGA) was performed on a LABSYS Evo TGDSC/DTA instrument (Setaram Instrumentation, France). Morphology and
40 chemical composition were measured by FEI Quanta 200 FEG SEM (Philips, The Netherlands) equipped with an energy-dispersive X-ray system. The N_2 adsorption-desorption isotherm was measured using an adsorption instrument (3Flex, Micromeritics, USA).

45 ### Synthesis of HKUST-1

HKUST-1 was prepared by a slightly modified solvothermal method [23]. 0.90 g of Cu$(NO_3)_2 \cdot 3H_2O$ was dissolved in 12 mL ultrapure water and mixed with 0.42 g of H_3BTC in 12 mL anhydrous ethanol. The resulting solution was sealed in a 50-mL
50 Teflon-lined stainless steel autoclave for 12 h at 120 ℃. After the solution was cooled, the solid product was collected by filtration, washed three times with ethanol and water, and vacuum dried at 60 ℃.

Synthesis of PCuS

55 10.0 mg of the HKUST-1 template and 5.0 equivalents of $Na_2S \cdot 9H_2O$ were suspended in 2.0 mL of ultrapure water. Then these two mixtures were mixed well and agitated overnight. The black product was collected by centrifugation, washed with water, and vacuum dried at 60 ℃.

60 ### Peroxidase-like activity of PCuS

The peroxidase-like activity of PCuS was investigated by catalytic oxidation of a peroxidase substrate, TMB, in the presence of H_2O_2. Solutions used for the kinetic analysis with TMB as the substrate consisted of 40 μL PCuS solution (2.5 mg
65 mL^{-1}), 30 mM H_2O_2, and varying concentrations of TMB (0, 0.2, 0.5, 0.8, 1.1, 1.4, 1.7 and 2.0 mM). Similarly, solutions used for the kinetic analysis of H_2O_2 as the substrate consisted of 40 μL PCuS (2.5 mg mL^{-1}), 1.4 mM TMB, and varying concentrations of H_2O_2 (0, 10, 20, 30, 40, 50, 60, and 70 mM). The kinetic
70 parameters were calculated based on Lineweaver−Burk plots of the double reciprocal of the Michaelis−Menten equation

$$1/V = K_m/V_{max}(1/[C]+1/K_m) \qquad (1)$$

where V is the initial reaction rate, V_{max} is the maximal reaction rate, C is the substrate concentration, and K_m is the Michaelis–
75 Menten constant.

Detection of Hg^{2+}

Standard solutions for the determination of Hg^{2+} were prepared as follows: 20 μL of PCuS solution (2.5 mg mL^{-1}) were added to 2.64 mL acetate buffer (0.2 M, pH 4.0). Specific volumes of
80 $HgCl_2$ stock solution were added to the PCuS-acetate buffer solutions to reach a final concentration. After standing for 15.0 min at room temperature, 200 μL of TMB (2.0 mM) and 140 μL H_2O_2 (5.0 wt %) were added to each solution. After these solutions stood at room temperature for 20 min, the absorption at
85 655 nm (A_{655}) signals were recorded for each solution using a Cary 60 spectrophotometer (Agilent, USA).

Hg^{2+} adsorption

All experiments were performed at room temperature (25 °C). 2.0 mg of PCuS were added into 4.0 mL Hg^{2+} solutions with different
90 concentrations. After adsorption for a pre-determined time, the supernatants were separated from the adsorbent by centrifugation (4500 rpm, 5 min) and analyzed for the concentration of Hg^{2+} according to a published procedure [24]. The adsorption capacity, q_e (mg g^{-1}), for Hg^{2+} was calculated using the following equation

95 $$q_e = (C_0 - C_e)V/m \qquad (2)$$

where C_0 (mg L^{-1}) and C_e (mg L^{-1}) is the initial and final concentrations of Hg^{2+}, respectively. V is the volume of Hg^{2+} solution (L), and m is the weight of PCuS (g).

Results and discussion

100 ### Characterization of PCuS

HKUST-1 is one of the most well-known and easily obtainable MOF, herein, HKUST-1 was prepared by a simple solvothermal method and then served as the precursor to synthesis PCuS. From HKUST-1 to PCuS, XRD, FT-IR, SEM and TGA etc.
105 characterization techniques were used to study the crystalline structures, functional groups, morphology and so on. Fig. 1 shows the XRD patterns for HKUST-1 and PCuS. Fig. 1a compares the diffraction peaks of the synthesized HKUST-1 with

a simulated one, indicating the successful preparation of HKUST-1. Fig. 1b presents the XRD pattern obtained for our synthesized PCuS using HKUST-1 as a precursor, and all the diffraction peaks consistent with the standard data of CuS (JCPDS card 78-2121). The diffraction peaks located at 27.70°, 29.21°, 31.85°, 32.78°, 48.01°, 52.68°, and 59.32° can be indexed to the (101), (102), (103), (006), (110), (108), and (116) planes of CuS, respectively. The strongest peak at (110) indicates the preferential growth direction 5, 25. The XRD results show that the HKUST-1 has been successfully transformed into CuS via a wet treatment method.
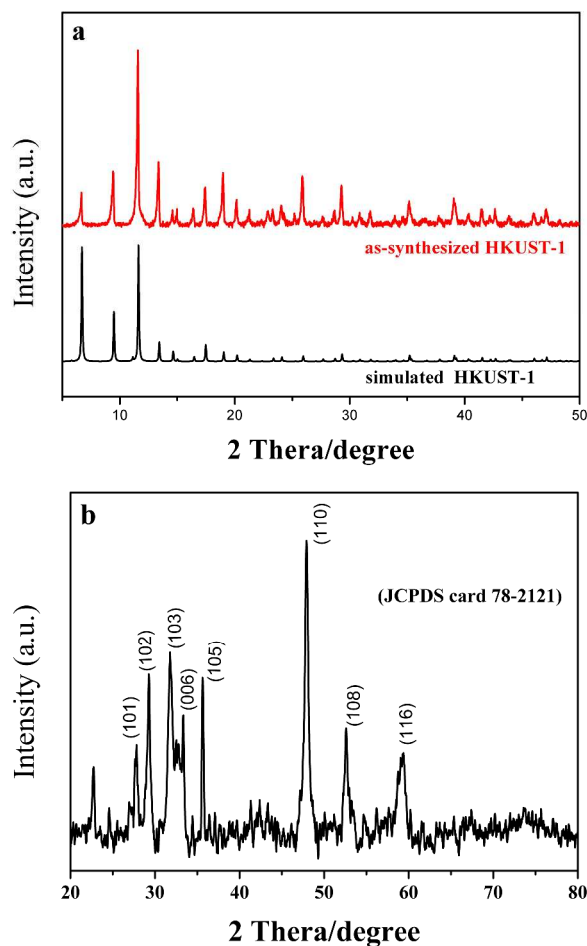

Fig. 1 XRD patterns of (a) HKUST-1, and (b) PCuS.

The morphology transformation from HKUST-1 to PCuS was investigated by SEM. Fig. 2 shows SEM images of HKUST-1, PCuS, and HKUST-1 together with PCuS. From these, it can be seen that the sulfidation reaction could induce an obvious change in morphology and the typical octahedral structure of HKUST-1 has disappeared and sphere-like particles have appeared and closely attached to each other, indicating an etching of HKUST-1 and the self-assembly of PCuS have occurred. These results suggest that the original organic linkages in HKUST-1 were exchanged by S^{2-}-layered bridges (further supported by FT-IR spectrum, Fig. S1) and formation of PCuS particles. When HKUST-1 and PCuS coexist (indicated by blue and red circles, respectively) in a solution and this solution is treated with Na_2S, PCuS particles self-assembled on the surface of the HKUST-1

crystal (Fig. 2d). This self-assembly event suggests that etching of HKUST-1 is from the surface of the octahedral structure crystals to the inner. The FT-IR spectra of HKUST-1 and PCuS are shown in Fig. S1. The peaks observed for HKUST-1 at 1642-1371 cm^{-1} were typical for the symmetrical stretching of bonds in the carboxylate groups in
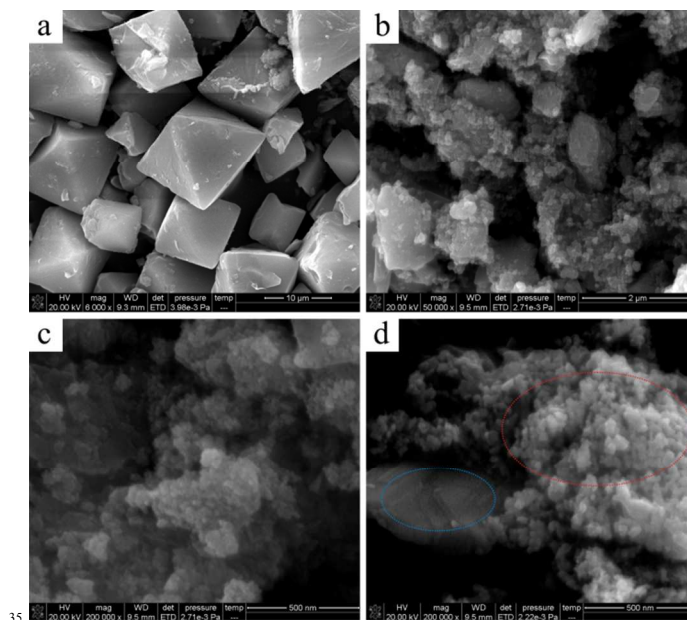

Fig. 2 SEM images of (a) HKUST-1, (b, c) PCuS, and (d) HKUST-1 and PCuS coexistence.

H_3BTC. The peaks at 728 cm^{-1} can be assigned to the Cu–O stretching vibration. For the PCuS sample, the characteristic peaks for H_3BTC and Cu–O almost disappeared (except for 1642 cm^{-1}), and new peaks at about 485 cm^{-1} appeared, resulting from Cu-S stretching. After Hg^{2+} adsorption, the peaks from Cu-S stretching decreased, which may be explained by the partial conversion of Cu-S to Hg-S. The Raman spectra of PCuS at 470 cm^{-1} for Cu-S also revealed that Hg^{2+} adsorption has reduced the quantity of Cu-S (Fig. S2).

The results from energy-dispersive spectroscopy (EDS) showed that PCuS contains 0.35% C, 14.52% O, 21.67% S and 62.6% Cu, respectively (Fig. S3a.). The presence of 0.35% C shows that H_3BTC, when exchanged by S^{2-} cannot be completed removed by washing (The result was also confirmed by its FT-IR). The elemental mapping revealed S and Cu were uniformly distributed in PCuS (Fig. S3b). The thermal stability of PCuS was investigated, and the TGA result is shown in Fig. S4. This result shows that coordinated water was driven off first. The second stage was caused by decomposition of residual H_3BTC, which could not be completely removed by washing. Last, it can be seen that the thermal decomposition of the S-bridging ligand occurs with the formation of CuO. Calculations using the TGA results show a copper content of 62% in PCuS. This number agrees well with the EDS analysis. The N_2 adsorption-desorption isotherms of PCuS is presented in Fig. 3, it could be seen that the PCuS was almost non-porous. However, the Brunauer–Emmett–Teller (BET) surface area of the PCuS was calculated to be 35 m^2 g^{-1}. This high surface area may be from the rough surface of PCuS and offers plenty of active sites for adsorption and can facilitate

catalytic reactions, which can result in better absorbing and catalytic performance. These results provide strong evidence that PCuS had been successfully synthesized.
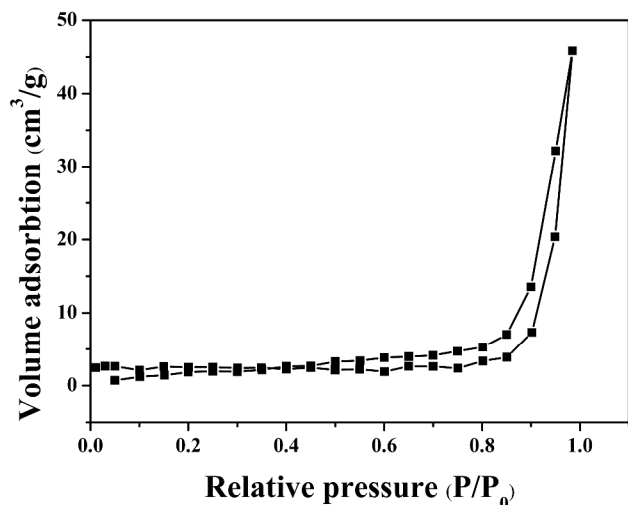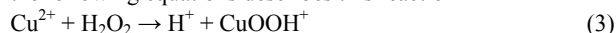

Fig. 3 N$_2$ adsorption-desorption isotherms of PCuS.

Peroxidase-like activity of PCuS

The peroxidase-like activity of PCuS was studied by catalytic oxidation of the peroxidase substrate, TMB, in the presence of H$_2$O$_2$. As shown in Fig. S5, only PCuS and H$_2$O$_2$ did not show
10 significant catalytic activity for TMB in an acetate buffer. In contrast, the TMB-H$_2$O$_2$ system in the presence of PCuS exhibited a strong absorbance at 655 nm, indicating that PCuS possesses remarkable peroxidase-like activity. The peroxidase-like activity might be due to the hydroxide radicals that were
15 produced by Fenton's reaction. A possible mechanism outlined in the following equations describes this reaction [26]

$$Cu^{2+} + H_2O_2 \rightarrow H^+ + CuOOH^+ \qquad (3)$$
$$CuOOH^+ \rightarrow HOO^\bullet + Cu^+ \qquad (4)$$
$$Cu^+ + H_2O_2 \rightarrow Cu^{2+} + OH\bullet + OH^- \qquad (5)$$

20 To better understand the peroxidase-like activities of PCuS, steady-state kinetic parameters for the reaction in TMB and H$_2$O$_2$ were determined. TMB and H$_2$O$_2$ concentration-dependent reaction rate curves are shown in Fig. 4. The curves display typical Michaelis−Menten behavior. By using a Lineweaver–
25 Burk plot, the Michaelis–Menten constant (K_m) and maximum initial velocity (V_{max}) values were obtained for both TMB and H$_2$O$_2$ (Table S1). These parameters showed that the synthesized PCuS possessed a high affinity for TMB and H$_2$O$_2$. This phenomenon benefited from the large surface areas and a wide
30 range of pore sizes in PCuS.

Hg^{2+} sensing

As displayed in Fig. 5, PCuS catalyzes the oxidation of the TMB-H$_2$O$_2$ solution, which led to the strong absorbance at 655 nm. However, when Hg^{2+} was added, the catalytic activity of PCuS
35 was dramatically inhibited. This inhibition of significant catalytic activity could be attributed to the extremely low K_{sp} value (2 × 10^{-52}) for HgS in conjunction with highly specific binding sites on the surface of PCuS. Hence, the active sites on PCuS were blocked, a phenomenon that is similar to catalyst poisoning.
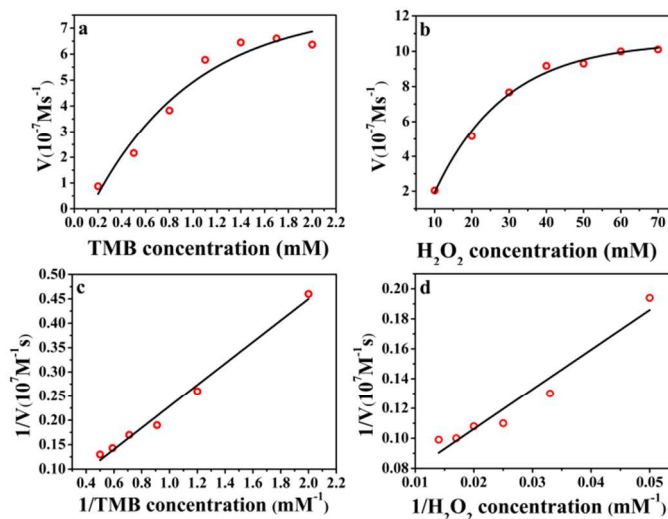40

Fig. 4 Plots of the steady-state kinetic calculations using the Michaelis–Menten model and Lineweaver–Burk model for PCuS: (a) and (c) varying [TMB] at a fixed [H$_2$O$_2$] (30 mM), (b) and (d) varying [H$_2$O$_2$] at a fixed
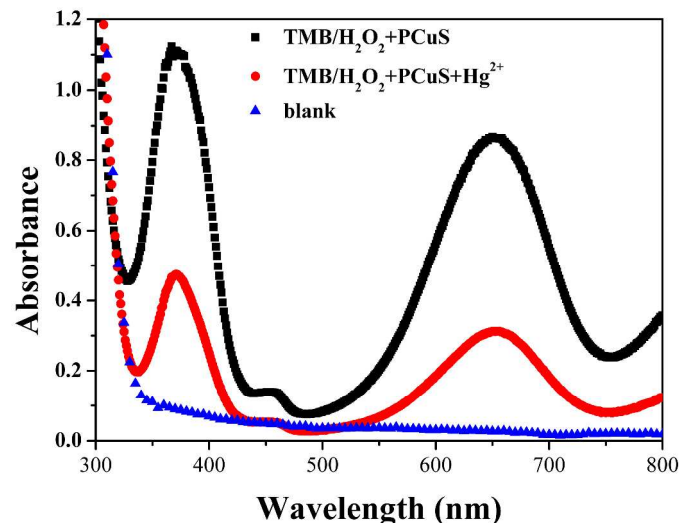45 [TMB] (1.4 mM).

Fig. 5 Absorption curves of the reaction products of TMB oxidation in the absence and presence Hg^{2+}.

As mentioned in Section 1, S atoms are essential for Hg^{2+} sensing
50 and absorption, so the amounts of Na$_2$S used in the fabrication of PCuS on the inhibition of Hg^{2+} were optimized. It was concluded from Fig. S6a, that five equivalents of Na$_2$S produced an optimal ΔA (ΔA = A$_0$− A, where A$_0$ and A were the absorbance intensities in the absence and presence of Hg^{2+}). All future work,
55 therefore, used 5.0 equivalents of Na$_2$S in the PCuS fabrication. The quantity of PCuS was also reviewed. As shown in Fig. S6b, 20 μL of the PCuS solution (2.5 mg mL^{-1}) produced the largest ΔA. Hence, all future work used 20 μL of the PCuS solution.

Using 20 μL of the PCuS solution, a series of solutions with
60 different concentrations of Hg^{2+} was analyzed. The results are shown in Fig. 6. A linear relationship between ΔA and [Hg^{2+}] over the concentration range of 3.0-40 μM (R=0.9899) was observed. The limit of detection (LOD) for Hg^{2+} (S/N=3) [27] was calculated to be 0.22 μM. After the completion of these
65 quantitative analyses, the method for adsorbing mercury ions was

reassessed. Different other metal ions were used to replace Hg^{2+}, as shown in Fig. S7. These ions were tested under the same experimental conditions as Hg^{2+}, and none of the metals was detected. The results indicated that the revised method had
5 excellent selectivity for Hg^{2+}. This selectivity was attributed to the very low K_{sp} value for CuS (6×10^{-36}). K_{sp} for CuS is much lower than other metal sulfides, even PbS (8×10^{-28}), so the control metal sulfides did not form on the surface of PCuS. To test whether our method was functional in real life applications,
10 pond water was tested through a standard addition method. As shown in Table S2, the recovery of Hg^{2+} was between 93.6 and 108%. These results indicated that this colorimetric method was applicable for the determination of Hg^{2+} in real samples.
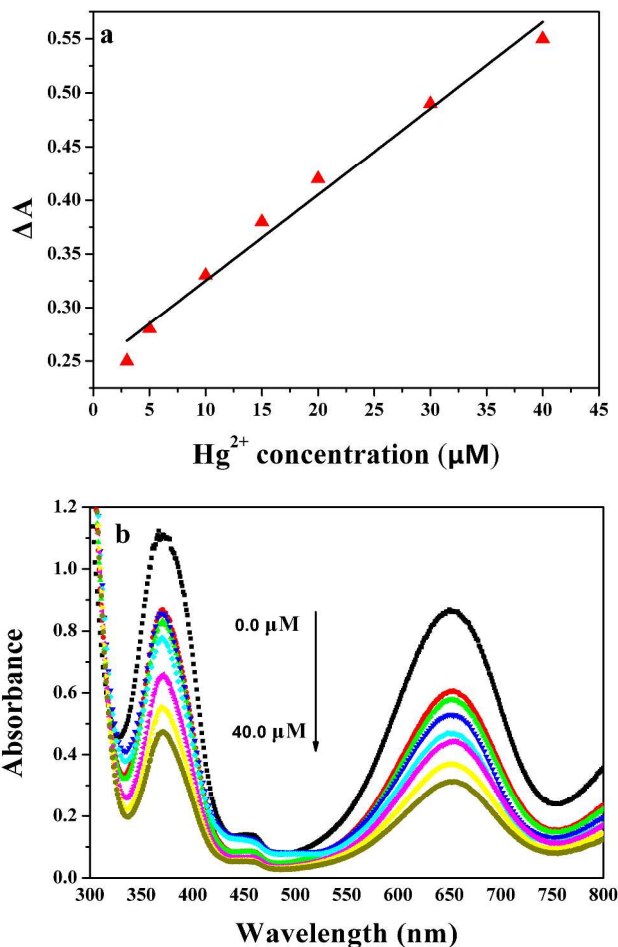
Fig. 6 Linear calibration of (a) the reaction system at varied Hg^{2+} concentrations, and (b) typical UV-vis spectra for the systems plotted in (a).

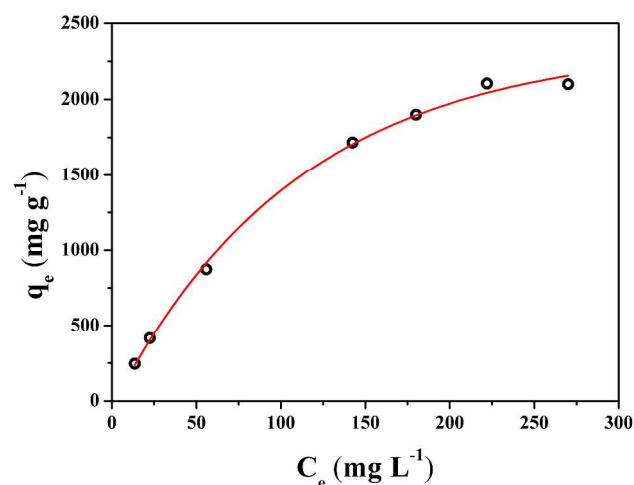### Hg^{2+} adsorption

20 For the Hg^{2+} adsorption test, adsorption isotherms and adsorption kinetics were chosen for understanding the mechanism of adsorption. As shown in Fig. 7, the adsorption amount gradually increased and then reached a platform with the increase in the concentration of Hg^{2+}. At equilibrium, the maximum adsorption
25 capacity of PCuS was 2105 mg g^{-1}. The equilibrium adsorption data were analyzed with the Langmuir adsorption model [28]

$$\frac{c_e}{q_e} = \frac{c_e}{Q_m} + \frac{1}{Q_m K_L} \tag{6}$$

where C_e (mg L^{-1}) is the equilibrium concentration, q_e (mg g^{-1}) is the equilibrium adsorption capacity, Q_m (mg g^{-1}) is the
30 maximum adsorption capacity, and K_L (L g^{-1}) is the Langmuir constant.

As shown in Fig. S8, a straight line was obtained when C_e/Q_e was plotted against C_e ($R^2=0.99$). This result indicated that the adsorption of Hg^{2+} conforms nicely to the Langmuir adsorption
35 model, showing monolayer coverage of Hg^{2+} on the surface of the PCuS [29]. Moreover, as presented in Table S3, the maximum adsorption capacity of PCuS was much higher than that reported previously, suggesting that PCuS possessed a superior adsorption capacity for Hg^{2+} [30-33].

Fig. 7 Equilibrium adsorption capacity Q_e versus equilibrium concentration C_e for the adsorption of Hg^{2+}.

Fig. 8 shows the effect of contact time on adsorption. The adsorption capacity of Hg^{2+} increased significantly in the first 45
45 min and then reached equilibrium. Adsorption kinetic characteristics were examined next. A pseudo-second-order model was used to fit the experimental data as follows [34]

$$\frac{t}{q_t} = \frac{1}{k_2 q_e^2} + \frac{t}{q_e} \tag{7}$$

where q_e and q_t are the adsorption capacities (mg g^{-1}) at
50 equilibrium and at time t (min), respectively, and k_2 is the rate constant for pseudo-second-order adsorption (g mg^{-1} min^{-1}).

The plot of Hg^{2+} using this pseudo second-order kinetic adsorption is shown in Fig. S9. The experimental data fit well with the pseudo second-order model ($R^2=0.99$). This result
55 implies that the rate-limiting step may be the chemisorption process [35].
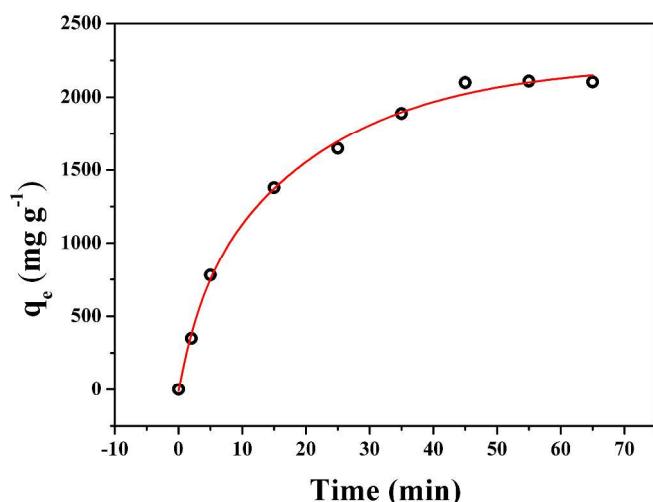
Fig. 8 Effect of contact time on adsorption of Hg^{2+} on PCuS.

For the desorption experiment, Hg^{2+} could not be eluted due to the strong binding force between Hg^{2+} and S^{2-}. However, considering the simple synthetic routes and high adsorption capacity of PCuS, the one-time use of the Hg^{2+} adsorbent will be likely acceptable.

Conclusions

In summary, CuS particles were successfully synthesized by wet treatment of HKUST-1 and used as a novel peroxidase-mimicking system for the colorimetric detection and efficient removal of Hg^{2+} from Hg-contaminated samples. The synthesized CuS particles showed several unprecedented advantages. First, the synthetic steps for producing CuS particles were simple and easy to perform. More importantly, using HKUST-1 as the precursor provided high surface areas for CuS particles. Second, based on the strong interaction between Hg^{2+} and S^{2-}, CuS particles played a role not only as a peroxidase-mimicking detector for Hg^{2+}, but also as an excellent adsorbent for Hg^{2+} removal. Notably, the outstanding adsorption capacity (>2100 mg g^{-1}) of Hg^{2+} has exceeded many other competing adsorbents. This work should facilitate the utilization of CuS in environmental abatement applications.

Acknowledgements

Notes and references

Key Laboratory for the Chemistry and Molecular Engineering of Medicinal Resources (Ministry of Education of China), College of Chemistry and Pharmaceutical Science of Guangxi Normal University, Guilin 541004, P. R. China.

Corresponding author: Prof. Fanggui Ye

Tel: +86-773-5856104; fax: +86-773-5832294

E-mail address: fangguiye@163.com

1. S. C. Riha, D. C. Johnson and A. L. Prieto, *J Am Chem Soc*, 2011, **133**, 1383-1390.
2. Y. Wu, C. Wadia, W. Ma, B. Sadtler and A. P. Alivisatos, *Nano Lett*, 2008, **8**, 2551-2555.
3. S. Goel, F. Chen and W. Cai, *Small*, 2014, **4**, 631-645.
4. W. He, H. Jia, X. Li, Y. Lei, J. Li, H. Zhao, L. Mi, L. Zhang and Z. Zheng, *Nanoscale*, 2012, **4**, 3501.
5. L. Mi, W. Wei, Z. Zheng, Y. Gao, Y. Liu, W. Chen and X. Guan, *Nanoscale*, 2013, **5**, 6589.
6. H. Furukawa, K. E. Cordova, M. O'Keeffe and O. M. Yaghi, *Science*, 2013, **341**, 1230444.
7. Y. Song, X. Li, L. Sun and L. Wang, *RSC Adv.*, 2015, **5**, 7267-7279.
8. S. Maiti, A. Pramanik and S. Mahanty, *Chem. Commun.*, 2014, **50**, 11717-11720.
9. W. Wang, Y. Li, R. Zhang, D. He, H. Liu and S. Liao, *Catalysis Communications*, 2011, **12**, 875-879.
10. S. J. Yang, S. Nam, T. Kim, J. H. Im, H. Jung, J. H. Kang, S. Wi, B. Park and C. R. Park, *J Am Chem Soc*, 2013, **135**, 7394-7397.
11. A. Banerjee, U. Singh, V. Aravindan, M. Srinivasan and S. Ogale, *Nano Energy*, 2013, **2**, 1158-1163.
12. C. Sun, J. Yang, X. Rui, W. Zhang, Q. Yan, P. Chen, F. Huo, W. Huang and X. Dong, *J. Mater. Chem. A*, 2015, **16**, 8483-8488.
13. C. W. Abney, J. C. Gilhula, K. Lu and W. Lin, *Adv Mater*, 2014, **26**, 7993-7997.
14. C. W. Abney, K. M. L. Taylor-Pashow, S. R. Russell, Y. Chen, R. Samantaray, J. V. Lockard and W. Lin, *Chem Mater*, 2014, **26**, 5231-5243.
15. G. Wu, S. He, H. Peng, H. Deng, A. Liu, X. Lin, X. Xia and W. Chen, *Anal Chem*, 2014, **86**, 10955-10960.
16. S. Kabiri, D. N. H. Tran, S. Azari and D. Losic, *ACS Applied Materials & Interfaces*, 2015, 969373680.
17. Z. Yan, M. Yuen, L. Hu, P. Sun and C. Lee, *RSC Adv.*, 2014, **4**, 48373-48388.
18. W. Li, B. Chen, H. Zhang, Y. Sun, J. Wang, J. Zhang and Y. Fu, *Biosensors and Bioelectronics*, 2015, **66**, 251-258.
19. Y. Deng, X. Wang, F. Xue, L. Zheng, J. Liu, F. Yan, F. Xia and W. Chen, *Anal Chim Acta*, 2015, **868**, 45-52.
20. L. Zhan, C. M. Li, W. B. Wu and C. Z. Huang, *Chem. Commun.*, 2014, **50**, 11526-11528.
21. G. Wang, L. Jin, X. Wu, Y. Dong and Z. Li, *Anal Chim Acta*, 2015, **871**, 1-8.
22. F. Ke, L. Qiu, Y. Yuan, F. Peng, X. Jiang, A. Xie, Y. Shen and J. Zhu, *J Hazard Mater*, 2011, **196**, 36-43.
23. K. Schlichte, T. Kratzke and S. Kaskel, *Micropor Mesopor Mat*, 2004, **73**, 81-88.
24. R. P. A. W. Paradkar, *Anal Chem*, 1994, **66**, 2752-2756.
25. A. K. Dutta, S. Das, S. Samanta, P. K. Samanta, B. Adhikary and P. Biswas, *Talanta*, 2013, **107**, 361-367.
26. Q. Cai, S. Lu, F. Liao, Y. Li, S. Ma and M. Shao, *Nanoscale*, 2014, **6**, 8117-8123.
27. L. Guo, Y. Xu, A. R. Ferhan, G. Chen and D. Kim, *J Am Chem Soc*, 2013, **135**, 12338-12345.
28. W. Xiao, P. Zhao, S. Deng and N. Zhang, *New J. Chem.*, 2015, **39**, 3719-3727.
29. Y. Li, S. Zhu, Q. Liu, Z. Chen, J. Gu, C. Zhu, T. Lu, D. Zhang and J. Ma, *Water Res*, 2013, **47**, 4188-4197.
30. L. Sun, Y. Li, M. Sun, H. Wang, S. Xu, C. Zhang and Q. Yang, *New J Chem*, 2011, **35**, 2697-2704.
31. S. Ravi, M. Selvaraj, H. Park, H. Chun and C. Ha, *New J Chem*, 2014, **38**, 3899-3906.
32. Y. Xie, B. Yan, C. Tian, Y. Liu, Q. Liu and H. Zeng, *J. Mater. Chem. A*, 2014, **2**, 17730-17734.
33. Z. Qu, L. Yan, L. Li, J. Xu, M. Liu, Z. Li and N. Yan, *ACS Applied Materials & Interfaces*, 2014, **6**, 18026-18032.
34. Q. Li, Z. Wang, D. Fang, H. Qu, Y. Zhu, H. Zou, Y. Chen, Y. Du and H. Hu, *New J. Chem.*, 2014, **38**, 248-254.
35. X. Zhao, D. Liu, H. Huang, W. Zhang, Q. Yang and C. Zhong, *Micropor Mesopor Mat*, 2014, **185**, 72-78.

New Journal of Chemistry Accepted Manuscript

Graphical abstract
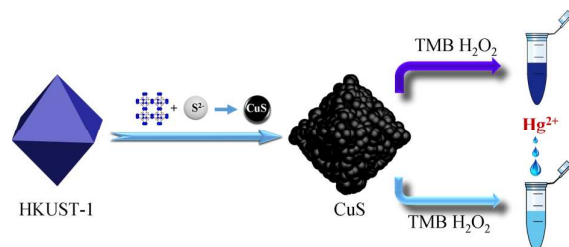
Table of Contents

From Cu-based metal organic framework to copper sulfide by wet-treatment: towards colorimetric determination and efficient removal of Hg^{2+}